Ser170 controls the conformational multiplicity of the loop 166–175 in prion proteins: implication for conversion and species barrier

Alemayehu A. Gorfe,[1] **and Amedeo Caflisch**

Department of Biochemistry, University of Zurich, Zurich, Switzerland

ABSTRACT   The self-perpetuating conversion of cellular prion proteins (PrP^C) into an aggregated β-sheet rich conformation is associated with transmissible spongiform encephalopathies (TSE). The loop 166–175 (L1) in PrP^C, which displays sequence and structural variation among species, has been suggested to play a role in species barrier, in particular against transmission of TSE from *cervids* to domestic and laboratory animals. L1 is ordered in elk PrP, as well as in a mouse/elk hybrid (in which L1 of mouse is replaced by elk) but not in other species such as mice, humans, and bovine. To investigate the source and significance of L1 dynamics, we carried out explicit solvent molecular dynamics simulations (≈0.5 μs in total) of the mouse prion protein, the mouse/elk hybrid, and control simulations, in which the mouse sequence is reintroduced into the structure of the mouse/elk hybrid. We found that the flexibility of L1 correlates with the backbone dynamics of Ser170. Furthermore, L1 mobility promotes a substantial displacement of Tyr169, rupture of the Asp178-Tyr128 and Asp178-Tyr169 side chain hydrogen bonds, as well as disruption of Tyr169-Phe175 π-stacking interaction. The simulation results go beyond the available experimental data because they highlight the dependence of this network of interactions on residue 170 and L1 plasticity.—Gorfe A. A., Caflisch A. Ser170 controls the conformational multiplicity of the loop 166–175 in prion proteins: implication for conversion and species barrier. *FASEB J.* 21, 3279–3287 (2007)

THE CELLULAR FUNCTION OF THE PRION PROTEIN (PrP) remains elusive (1, 2), despite extensive investigations spurred by the association of PrP with fatal diseases called transmissible spongiform encephalopathies (TSEs) or "prion diseases" (1, 3, 4). TSEs include bovine spongiform encephalopathy (BSE), Creutzfeldt–Jakob disease in humans, feline spongiform encephalopathy, scrapie in sheep, and chronic wasting disease (CWD) in *cervids*. The protein-only hypothesis states that the major component, if not the only one, of the infectious particle causing TSE is the aggregated "scrapie" isoform (PrP^{Sc}) (1, 4–6). The transition from the cellular α-helical PrP^C to the infectious β-sheet-enriched PrP^{Sc} occurs by conformational change, and subsequent propagation arises from the ability of PrP^{Sc} to transmit its conformation to the neutral isoform. In support of the protein-only hypothesis, structural models of PrP^{Sc} are providing useful insights into how seeded β-sheets organize to the disease-causing fibril (7–10).

The incubation time for onset of TSEs from cross-species infection is prolonged as compared to the transmission of infectious material within the same species, indicating species barrier (11–15). The heterogeneity and low availability of purified infectious material considerably limits structural investigations of PrP^{Sc} from diverse species. As a result, little is known about how the apparently sequence-dependent species barrier occurs. On the other hand, analysis of NMR structures of recombinant PrP^C from several species helped identify structural features that may play a role in species barrier (16–22). The overall structure of PrP^C is similar across species with the first 120 amino acids being disordered and the second half of the protein adopting a globular domain that has three α-helices and an 8-residue two-stranded antiparallel β-sheet (**Fig. 1,** left). Nonetheless, localized structural variations have been observed (16–21, 23, 24).

Considering the stringency of the barrier against the transmission of CWD from *cervids* (including elk) to domestic mammals (25, 26), the availability of the elk prion protein (ePrP) NMR structure (19) and the structure of other PrPs has been particularly useful. Such a comparison revealed that the loop connecting β2 and α2 (residues 166–175, L1) is precisely defined in ePrP, while it exhibits pronounced structural disorder in PrP^C of other species, such as mice, humans, bovine, cats, and dogs (18–20).

The ePrP has two amino acid substitutions at positions 170 and 174 of L1 when compared to the mouse (mPrP) and bovine (bPrP) sequences (Fig. 1, right). Introduction of the L1 sequence of ePrP into mouse
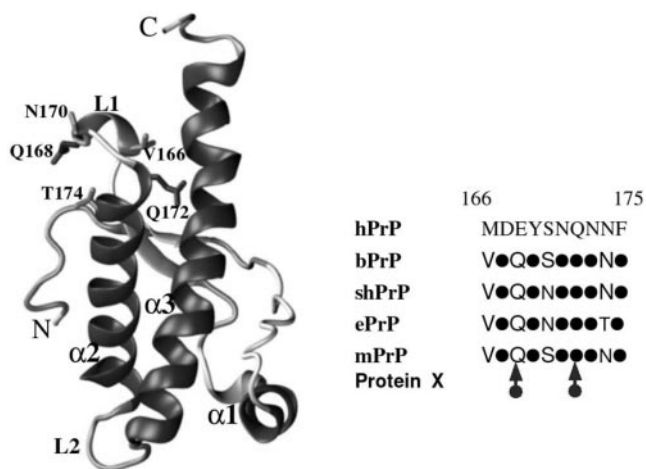
Figure 1. Left: Ribbon representation of the NMR structure of the mouse/elk hybrid S170N/N174T. The short β-sheet comprising strand β1 (residues 128–131) and β2 (residues 161–164) is at the back, whereas helices α1 (residues 143–153), α2 (residues 172–191) and α3 (residues 199–227) are in front. The definition of structural elements is as described in ref. 19. Right: Amino acid sequences of the loop 166–175 (L1) in human (hPrP), bovine (bPrP), Syrian hamster (shPrP), elk (ePrP) and mouse (mPrP) prion proteins. Conserved amino acids are represented by solid circles (the hPrP is used as a reference). The binding sites for the hypothetical chaperone "protein X" are shown by arrows.

(≡ mouse/elk hybrid, mPrP[S170N,N174T]) (19) resulted in a structured loop that exactly mimics ePrP, showing that the structured loop in ePrP relates to these two local amino acid exchanges. Furthermore, Syrian hamster prion protein (shPrP) (22), which carries an Asn at position 170 and a designed S170N variant of human PrP (19), have a partially stabilized L1. The structure of L1 in the mouse N174T variant is characterized by the same slow conformational exchange as in the wild-type mPrP (19). Thus, Ser170, especially in conjunction with Asn174, appears to dictate the structural stability of L1 in PrP[C]. Interestingly, in this context, L1 residues 168 and 172, together with residues 215 and 218 at the C-terminal half of α3, are proposed to form a disease-related epitope for the binding of the hypothetical "protein X" (27). These two segments are also the binding sites for a monoclonal antibody (28). Furthermore, the two regions experience the largest sequence variation among mammalian species (16), as well as between mammalian and avian PrPs (18).

To investigate the origin and consequence of L1 dynamics, we carried out explicit solvent molecular dynamics (MD) simulations of the mPrP (residues 120–232), the mouse/elk hybrid (mPrP[S170N,N174T]), and control simulations in which the mouse sequences were reintroduced into the structure of the mouse/elk hybrid. We observe that the flexibility of L1 is a result of the backbone conformational dynamics of Ser170. Furthermore, L1 mobility results in Tyr169 side chain displacement, rupture of Asp178-Tyr128 and Asp178-Tyr169 side chain hydrogen bonds, as well as loss of Tyr169-

Phe175 π-stacking interaction. We also observe dynamic interactions between Ser170 and the C-terminal end of α-helix 3 in the context of flexible L1. The implications of the results to conformational conversion and species barrier are discussed.
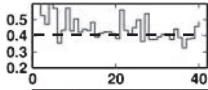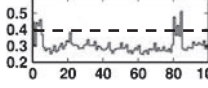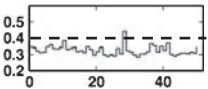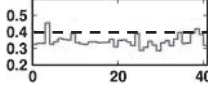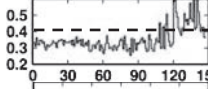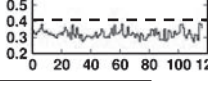
MATERIALS AND METHODS

Explicit solvent molecular dynamics simulations at physiological temperature (310 K) were performed for a total of 0.5 μs (**Table 1**). The charge assignments reflect the moderately acidic (pH=4.5) condition of the NMR experiments; based on calculated pK_as averaged over all the NMR conformers (29), all aspartate, glutamate, histidine, arginine, and lysine residues were in their charged forms. The CHARMM force field (30) and TIP3P water model were used in all simulations. The programs CHARMM (31) and NAMD (32) were used for setup (minimization and equilibration) and dynamics, respectively. The simulations were carried out following the protocols described before (33), using particle mesh Ewald treatment of electrostatics and a cutoff of 12 Å for van der Waals. The "species" studied here include the wild-type mouse (mPrP, PDB code 1XYX (19)), mouse/elk chimera in which L1 of mouse has been substituted by that of an elk through S170N/N174T double mutation (mPrPel, PDB code 1Y16 (19)), and reverse-mutations (mPrPmb) in which simulations are started from the structure of the mouse/elk hybrid with the two amino acids of the elk sequence (Asn170 and Thr174) mutated back to the wild-type mouse sequence (Ser170 and Asn174). For each species, that is, mPrP, mPrPel, and mPrPmb, two simulations were run, differing only in the assignment of initial velocities, to improve sampling. Note that long simulations were preferred (Table 1) over multiple short runs in order to reduce the dependence on the initial NMR conformer, in particular for the mutants with modeled side chains.

RESULTS

Values of the root mean square deviation (RMSD) averaged over the last 20 ns of each simulation are listed in Table 1. As observed in previous simulations (*e.g.*, (34)), the all-residue RMSDs are somewhat high due to the substantial conformational changes at the terminals and loops. When only the regular secondary structure elements are considered, the RMSD reduces by up to 65%, especially in simulations started from the mouse/elk hybrid PrP, which has a better defined NMR structure. To illustrate this relative flexibility, superposition of snapshots collected at 100-ps intervals along the 150-ns simulation of mPrPmb is shown in **Fig. 2**, top. The displacements at the termini and loops β1–α1, β2–α2 (L1) and α2–α3 (L2) account for a large part of the total deviation from the starting structure, while helix α1 undergoes a mainly rigid-body motion. A similar rigid-body displacement of α1 was observed first in MD simulations (35) and then by NMR analysis (18).

The root mean square fluctuations are similar in all simulations (Fig. 2, bottom). The largest difference is at L1, where a substantially increased mobility is observed in one of the two mPrP runs and one of the two

TABLE 1. *Simulations performed and L1 flexibility analysis*

| Name | L1 sequence (166-175) | PDB code | Length [ns] | Cα-RMSD [Å][a] | | D178 interactions[b] | | L1 fluctuation[c] |
				all	Sec. str.	Y128	Y169	
mPrP	mouse VDQYSNQNNF	1XYX	41	2.8±0.2	2.4±0.2	−	−	
			100	3.2±0.1	2.5±0.2	+	+	
mPrPel	mouse/elk hybrid VDQY**N**NQN**T**F	1Y16	51	2.3±0.3	1.6±0.2	+	+	
			40	2.7±0.3	1.9±0.2	+	+	
mPrPmb	mouse (back mutation) VDQYSNQNNF	1Y16	150	2.3±0.2	1.5±0.2	±	−	
			120	1.9±0.2	1.3±0.2	±	±	

[a] Cα-RMSD of residues 125–227 and regular secondary structure elements (see Fig. 1, left, for definition of α-helices and β-sheet). Values of Cα-RMSD are averages over the last 20 ns of each simulation. [b] Presence (+), absence (−), or fluctuation (±) of hydrogen bonding interactions (donor-acceptor distance cutoff 3.5 Å) between side chain functional groups of Asp178 with Tyr128 or Tyr169. [c] Time evolution of the root mean square fluctuation (RMSF, y-axis) computed over each nanosecond and averaged over residues 166–175. The dashed line at RMSF = 0.4 Å helps in defining the loop 166–175 (L1) as flexible (above line) or rigid (below line). RMSFs were calculated after optimal superposition of L1 Cα atoms only.

mPrPmb runs. Interestingly, the simulations suggest an anticorrelation between the flexibility of L1 and the stability of a hydrogen bond network involving side chains of residues Tyr128, Tyr169, and Asp178 (Table 1). As will be shown below, these interactions, together with a Asp178-Arg164 salt bridge and a Tyr169-Phe175 π-stacking interaction, stabilize long-range contacts between the N-terminus of β1 (Tyr128), the C-terminus of β2 (Arg164), the middle of L1 (Tyr169), and the N-terminal part of α2 (Phe175 and Asp178). Independent of the structural definition of L1 in the starting conformation (compare simulations mPrP and mPrPmb), dynamics and/or conformational change of L1 led to a meltdown of these interactions.

Another interesting observation is that in the simulations in which L1 is stable, the C-terminal region comprising residues 222–232 is also less mobile (Fig. 2, bottom). This finding suggests that the amino acid exchanges at L1 modulate the structure and/or dynamics of the two so-called conformational markers, 166–172 and 215–230 (17, 27). To further examine the correlation between the motion of L1 and helix α3, the cross-correlation coefficients between the displacements of each pair of residues were calculated. A correlated motion between L1 and helix α3 is observed in all simulations, excluding the N-terminal part of

helix α3 (residues 199–210) in simulations with ordered L1 (Supplemental Fig. S1).

DISCUSSION

Loop 166–175 is flexible in mouse PrP but not in mouse/elk hybrid PrP

The mobility of L1 in the nanosecond time scales is smaller in the mouse/elk hybrid (PrPel) than in the mouse (mPrP and mPrPmb) simulations (Table 1 and Fig. 2, bottom). In half of the mPrP and mPrPmb runs, the L1 loop was very flexible. That L1 is ordered for up to 100 ns in the other half (*e.g.*, cyan in Fig. 2, bottom) indicates existence of at least two conformations slowly exchanging with one another. This is consistent with the slow conformational exchange for mPrP as suggested by NMR (19, 24). Further, in the case of mPrPmb, it is to be expected that the reintroduced amino acids would need time to locally rearrange. Thus L1 did not undergo a substantial conformational change until 120 ns but experienced an enhanced mobility in the range 120–150 ns in the longer simulation. On the other hand, one of the mPrP simulations quickly converted into the stable L1 geometry and remained ordered for the 100ns duration of the simulation.
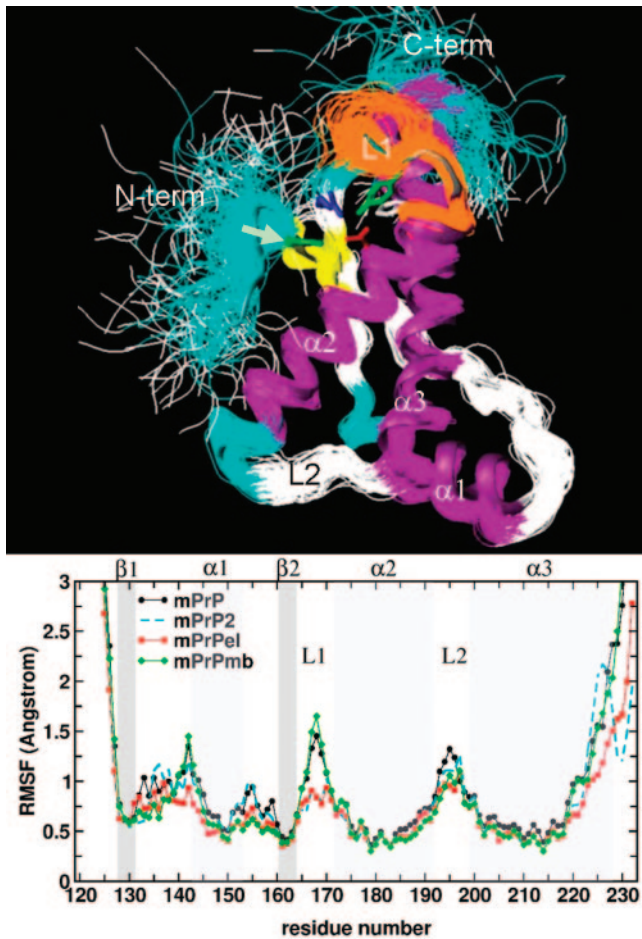
Figure 2. Backbone fluctuations. Top: Snapshots collected at 100-ps interval along simulation mPrPmb are superposed (lines) onto the equilibrated starting conformation (cartoons, PDB code 1Yl6). Structures were fitted using all Cα atoms, except the terminal five residues. The loop 166–175 (L1) is shown in orange. Residues (clockwise from the arrow) Tyr128 (green), Arg164 (blue), Tyr169 (green), Phe175 (gray), and Asp178 (red) are shown in a stick model. All except Phe175 side chains are involved in a hydrogen bond network in PrP structures having an ordered L1, while Phe175 contributes to the stability of L1 through π-stacking interaction with Tyr169. For a better view of these residues, the figure was slightly rotated relative to Fig. 1A. Bottom: Cα root mean square fluctuation (RMSF) calculated at 1-ns interval and averaged over the last 20 ns of the simulations. The RMSF for run 2 of mPrPel and mPrPmb are similar to run 1 of mPrPel.

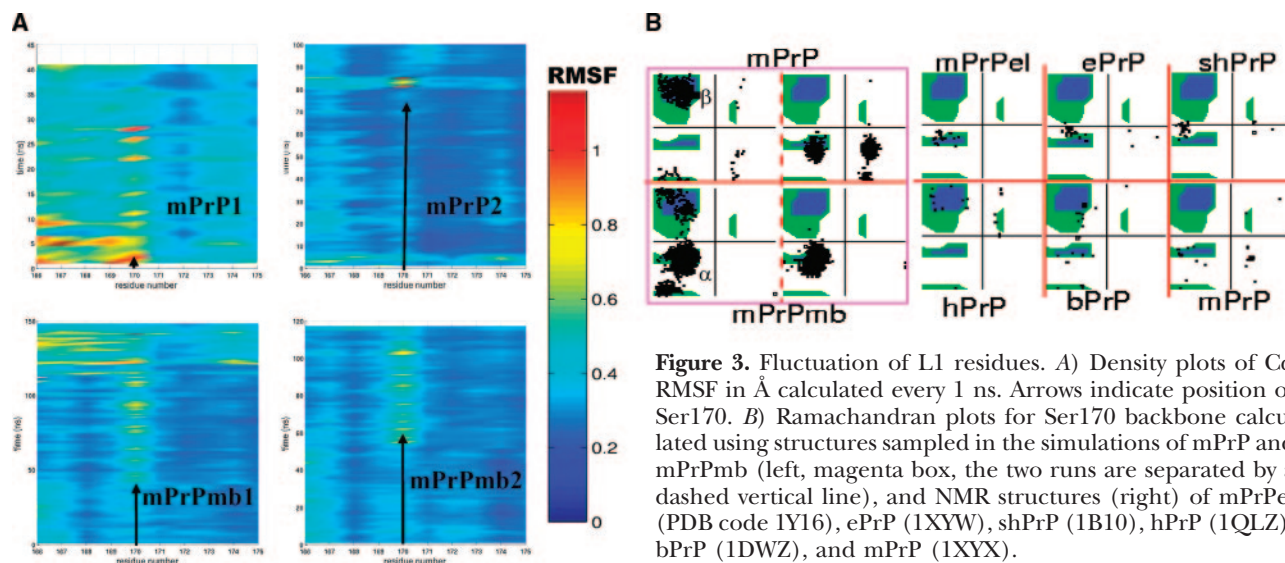## Ser170 is responsible for the conformational dynamics of loop 166–175

Ser170 is a "hot spot" in all of the simulations containing the wild-type L1 sequence (**Fig. 3A**), but there is no sign of Asn170 mobility in mPrPel (not shown). A closer inspection of Fig. 2B and Fig. 3A reveals that the backbone dynamics of Ser170 extends to residues 166–169. Furthermore, the time evolution of the fluctuations suggests that it takes tens of nanoseconds for the motion to propagate from the hot spot Ser170 to the N-terminal part of L1 (*i.e.,* residues 166–169), as is the

case in the longest simulation (Fig. 3A). Residues 172–175 are less mobile, with Asn174 becoming only slightly flexible following a conformational change in L1 (Fig. 3A). In fact, there is no significant difference between the flexibilities of Asn174 in mPrP and Thr174 in mPrPel (not shown), consistent with the NMR data, which indicated that in contrast to the double mutant, the N174T mutation alone did not alter the structural definition of L1 in mPrP (19).

How does the conformation of Ser170 backbone change? Fig. 3B shows Ramachandran plots (*i.e.,* the ϕ/ψ dihedral angles) of Ser170 for snapshots sampled every 100 ps of simulations mPrP and mPrPmb. Conformational exchange is observed for mPrP and one of the two runs of mPrPmb between regions of the (generously defined) right handed α-helix and extended conformations. In contrast, the dihedral angles of Asn170 in mouse/elk hybrid populate only the α-helix region of conformational space (not shown). The same plots for the NMR conformers from the protein databank (PDB) indicate that the ϕ/ψ angles in mouse/elk hybrid (mPrP[S170N,N174T], mPrPel) and ePrP populate only the α-helical conformation. The lack of disorder is in contrast with the distribution in the NMR conformers of hPrP, bPrP and mPrP, which scatter in a similar manner as in simulations of mPrP and mPrPmb. The dihedrals in shPrP have an intermediate structural variation.

The L1 flexibility increases significantly when Ser170 switches from the α-helical to the extended region of the Ramachandran map. In the NMR structures, L1 is structured in ePrP and mPrPel, partially structured in shPrP and disordered in hPrP, bPrP, and mPrP (19). Thus, in both the simulations and the NMR structures, the Ser170 dihedral angle distribution directly reflects the mobility of L1. Taken together, the simulation results and NMR conformers indicate not only the existence of, and slow exchange between, multiple conformations of L1 in mammalian PrPs that carry a Ser at position 170 but also that the L1 flexibility is governed by the conformation of Ser170 itself. Furthermore, the effect of an Asn/Ser exchange depends on the exact location in L1, as the pig prion protein (scPrP)—which has a Ser at position 173 instead of Asn—has an ordered L1 (20). It is worth noting here that the distance between the proposed "Protein X" binding surface residues at L1, Q168, and Q172 (27), increases by ~2 Å upon the conformational change of L1. The energetic consequences of Ser170 conformational change and its major interactions will be discussed in a later section.

Using sequence comparison and analysis of available NMR structures, Dima and Thirumalai suggested that the C-terminal segment of α2 is frustrated in the helical state and might play a role in the α-to-β transition (36). Although it is difficult to relate their analysis with the present simulation study, it has to be noted that residues 170 and 174 were identified by the same authors among the residues with unsatisfied buried hydrogen-bond donors/acceptors in mammalian prion proteins (36).

Figure 3. Fluctuation of L1 residues. *A*) Density plots of Cα RMSF in Å calculated every 1 ns. Arrows indicate position of Ser170. *B*) Ramachandran plots for Ser170 backbone calculated using structures sampled in the simulations of mPrP and mPrPmb (left, magenta box, the two runs are separated by a dashed vertical line), and NMR structures (right) of mPrPel (PDB code 1Y16), ePrP (1XYW), shPrP (1B10), hPrP (1QLZ), bPrP (1DWZ), and mPrP (1XYX).
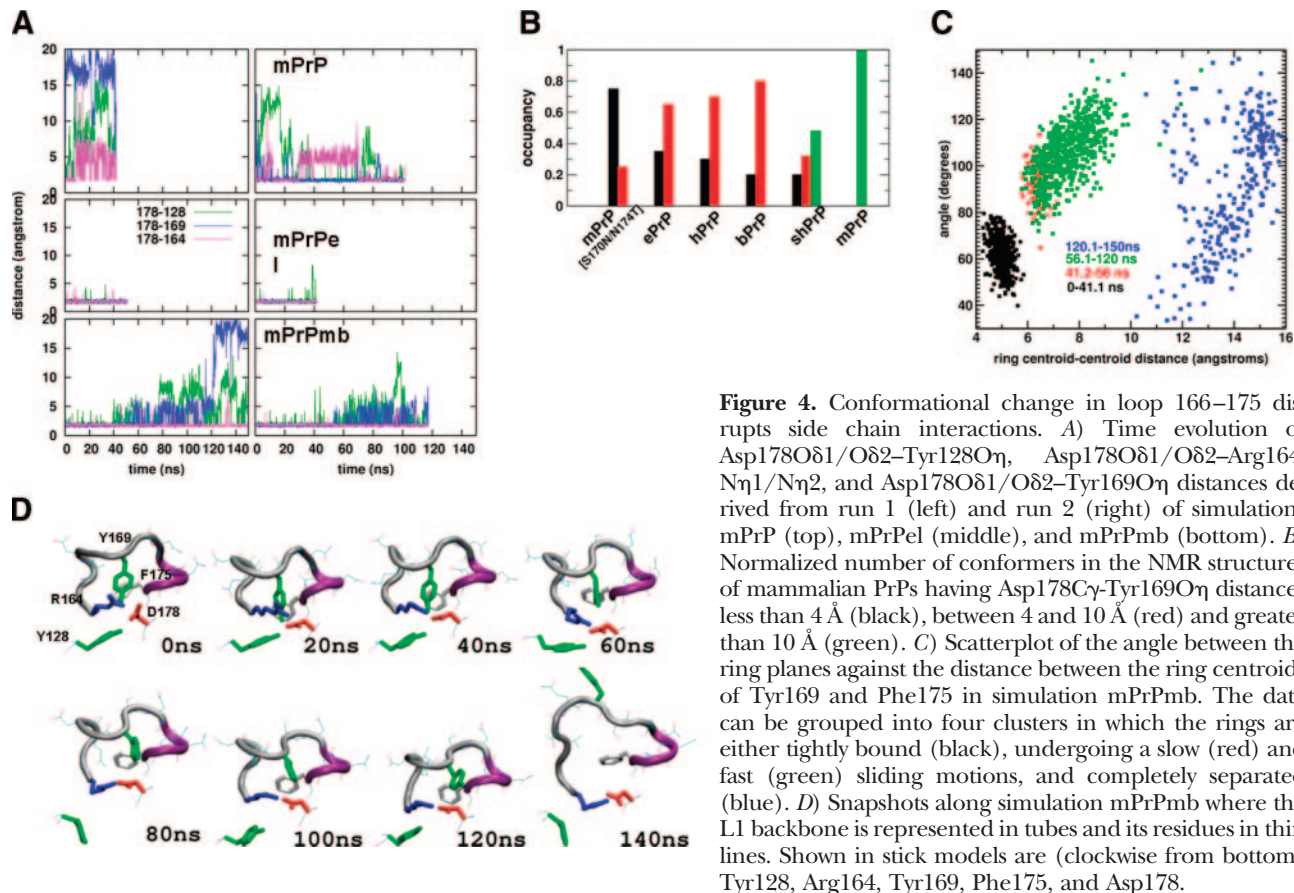
Rupture of hydrogen bonding and hydrophobic interactions

Several hydrogen bonding and hydrophobic interactions are disrupted as a result of the L1 conformational change; specifically, Tyr128-Asp178 and Tyr169-Asp178 side chain hydrogen bonds and Tyr169-Phe175 π-stacking interaction are invariably broken (**Fig. 4**).

The loss of the hydrogen bond involving Tyr169 is concomitant with the conformational change of L1

(compare Figs. 3*A* and 4*A*). Because Tyr169 lies in the middle of L1, it is reasonable that its side chain orientation is affected by the structure of L1. Indeed, analysis of NMR structures of several species shows that with the possible exception of shPrP, the structural definition of L1 is proportional to the number of conformers having the side chains of Tyr169 and Asp178 in contact (Fig. 4*B*), an important observation so far overlooked. Furthermore, the Tyr169Oη-Asp178Cγ distance is greater than 10 Å in all of the

Figure 4. Conformational change in loop 166–175 disrupts side chain interactions. *A*) Time evolution of Asp178Oδ1/Oδ2–Tyr128Oη, Asp178Oδ1/Oδ2–Arg164-Nη1/Nη2, and Asp178Oδ1/Oδ2–Tyr169Oη distances derived from run 1 (left) and run 2 (right) of simulations mPrP (top), mPrPel (middle), and mPrPmb (bottom). *B*) Normalized number of conformers in the NMR structures of mammalian PrPs having Asp178Cγ-Tyr169Oη distances less than 4 Å (black), between 4 and 10 Å (red) and greater than 10 Å (green). *C*) Scatterplot of the angle between the ring planes against the distance between the ring centroids of Tyr169 and Phe175 in simulation mPrPmb. The data can be grouped into four clusters in which the rings are either tightly bound (black), undergoing a slow (red) and fast (green) sliding motions, and completely separated (blue). *D*) Snapshots along simulation mPrPmb where the L1 backbone is represented in tubes and its residues in thin lines. Shown in stick models are (clockwise from bottom) Tyr128, Arg164, Tyr169, Phe175, and Asp178.

mPrP NMR conformers, consistent with the substantial displacement of Tyr169 side chain in the simulations. The other interaction that has a direct correlation with the motion of L1 (or Ser170, Fig. 3A) is the Tyr169-Phe175 π-stacking interaction. As an example, the relative position of the two aromatic rings in simulation mPrP, as measured by the distance between the ring centroids, as well as by the closest distance between relative carbon atoms, is shown in Fig. S2. When compared with the equivalent values R_{cen} and R_{clo} obtained from a representative set of high-resolution X-ray structures (37), there exists a strong π-stacking interaction until ~41ns, which then gets weaker and eventually lost. The scatterplot of the angle between the two vectors connecting the ring center with the Cζ atom against the distance between the centers of the rings shown in Fig. 4C indicates a stepwise Tyr169/Phe175 unstacking; such as tight (~4.5 Å) to intermediate (~6.5 Å) interaction between the rings, followed by sliding motions (~6.5–10 Å) to complete separation.

The snapshots in Fig. 4D illustrate the concerted displacements: Tyr169 and Phe175 phenyl rings slide and rotate relative to each other but remain close as long as the orientation of Tyr169 side chain is maintained by its hydrogen bond with Asp178 (up to ~41 ns, Fig. 4A, D). Thus, the latter helps stabilize the relatively malleable hydrophobic interaction between the rings. However, these interactions are apparently not strong enough to withstand the L1 conformational change induced by the rotation of Ser170.

"Allosteric" effect of loop 166–175 in its extended conformation

While the van der Waals and electrostatic interactions of the Ser170 side chain with the rest of the protein do not change significantly, the electrostatic interaction energy of its backbone improves by ~2 kcal/mol upon the conformational change in L1 (**Fig. 5**, dashed and solid lines).

To investigate the reason for the enhanced electrostatic interaction of Ser170 backbone on the conformational change, i.e., the α-to-β transition in the Ramachandran plot (Fig. 3B), the heavy atoms dynamically approaching residues 170 and 174 were identified (cutoff 4 Å). Examples are displayed in **Fig. 6** from mPrPmb. Interestingly, besides the sequence neighbors, Ser170 in its extended conformation interacts with atoms at the C-terminal half of helix α3. Perhaps the most important is the proximity and occasional hydrogen bonding between Tyr218 hydroxyl and Ser-170 backbone carbonyl. The interaction is rather dynamic, reflecting the mobility of both segments, but since residue 218 is part of the protein X epitope (27) and is involved in antibody binding (28), its interaction with L1 may have implications in the structural properties of both the cellular and scrapie forms of PrP. Furthermore, the fact that helix α3 is better defined in
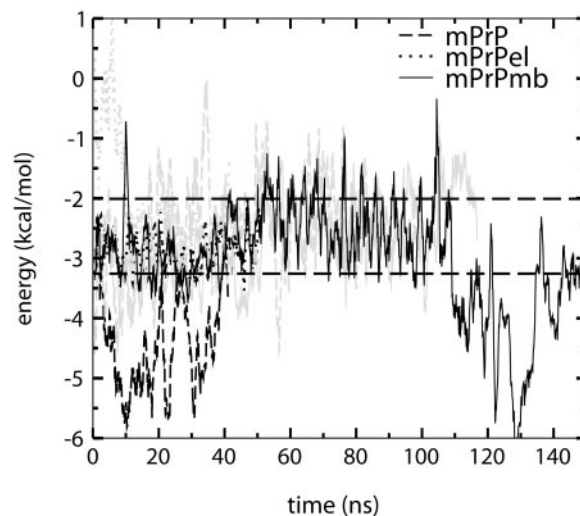

Figure 5. Interactions of Ser170. Time evolution of the electrostatic interaction energy between the backbone atoms of Ser170 and the rest of the protein is shown. The dashed lines roughly demarcate the range in which the energy fluctuates in an ordered L1. Gray lines represent the second trajectory of a pair.

the ePrP than in mPrP (and other mammals with Ser at 170) may be partly explained by a flexibility-based "allosteric" effect of L1 on α3.

Implications of loop 166–175 dynamics to species barrier and PrP^C–PrP^Sc conformational change

The current understanding of species barrier is limited because the heterogeneity and low availability of the infectious species generated in vivo or in vitro considerably restrict structural investigations of PrP^Sc. However, useful insights have been gleaned from comparative analysis of PrP^C structures derived from a variety of sources (16–21, 23, 24).

The role of L1 in species barrier becomes apparent when considering the transmission of chronic wasting disease (CWD) between cervides and other mammals (38). CWD affects captive and free-ranging elk (Cervus elaphus nelsoni) (39–41), captive mule deer (Odocoileus hemionus), and white-tailed deer (O. virginianus) (38, 42, 43). It appears to be propagated through direct or environmental contamination (26, 44, 45). However, unlike BSE, the transmission of CWD to domestic animals, such as cattle, goats, and laboratory animals, was found to be inefficient, suggesting that there is a rather stringent species barrier (25, 26). On the other hand, cell-free conversion experiments predicted similar transmission efficiency of TSE from cervids to humans as from cattle to humans (46). Notably, L1 is part of the hypothetical "protein X" epitope (27), polymorphism at positions 168 and 171 in ovine PrP causes a varying level of scrapie susceptibility (47, 48) and that peptides corresponding to residues 166–179, as well as 200–223, inhibit PrP^C–PrP^Sc conversion (49). Therefore, the higher flexibility of loop 166–175 in the
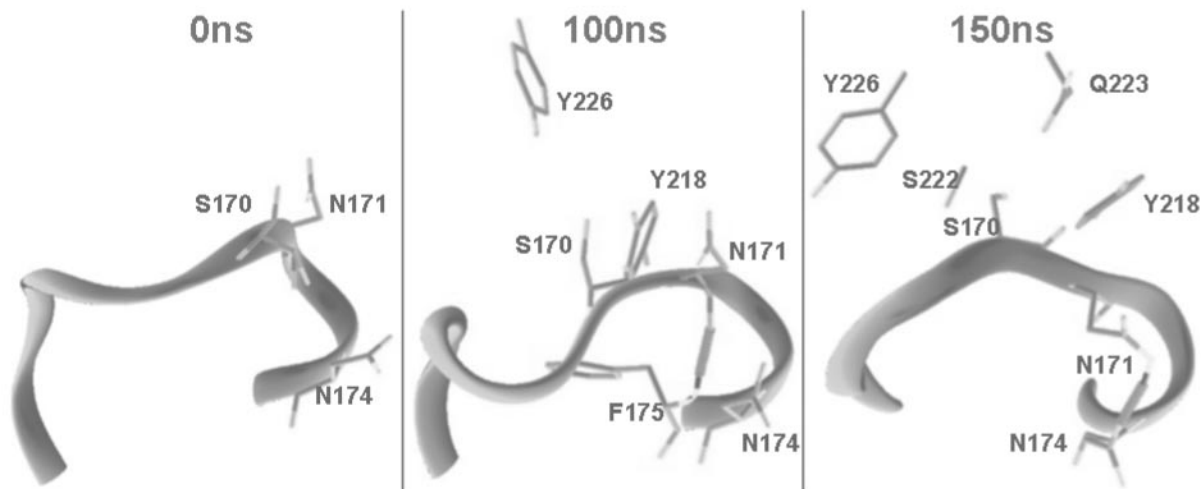
Figure 6. Dynamic contacts of helix α3 side chains with L1. Snapshots at 0, 100, and 150 ns along simulation mPrPmb showing (in sticks) side chains in helix α3 that are within 4 Å of any heavy atom of Ser170 or Asn174. Hydrogen bonds of Asn171 are emphasized in thick lines.

mouse than mouse/elk hybrid, which strongly suggests existence of two or more conformational states of L1 slowly exchanging with one another, might play a role in species barrier between mouse and elk, or between *cervids* and other mammals in general. Structural and dynamic alterations caused by the conformational change at L1 may have additional implications. For example, the network of interaction Tyr128-Arg164-Tyr169-Phe175-Asp178 connects far flung sections of the structure, including the N-terminal residues 120–176—a segment likely to be involved in the conformational change to the fibril forming β-sheet (7)—to the rest of the protein. The loss of the network could facilitate the conformational conversion. Notably, it has been suggested that the electrostatic interaction between Asp178 and Tyr128 side chains inhibit conformational changes of PrP^C, its loss facilitating addition of another strand to the β-sheet (50). Note also that polymorphisms at positions 129 and 178, such as the D178N, are associated with the variant Creutzfeldt–Jakob disease (51).

To summarize, the MD simulations identify in the Asn170Ser substitution the origin of the destabilization of L1 in mPrP compared with the mouse/elk hybrid, and the generality of the results was demonstrated by analyzing the NMR structures of several species, including humans. Taken together, the results indicate that Ser170 backbone dynamics causes L1 mobility, which is associated with the rupture of side chain hydrogen bonds between Asp178 and Tyr128/Tyr169, as well as loss of Tyr169-Phe175 π-stacking interaction. These interactions contribute to the structural stability of the L1 loop in the elk sequence. Thus, the simulation results extend the available experimental observations not only by providing details inaccessible to experiments, but also by directly connecting the structural mobility at L1 to disturbances of networks of atomic interactions, as well as side chain displacements. The resulting implications for the PrP^C–PrP^{Sc} transition suggest that L1, and residue 170 in particular, is a crucial target for future investigations of species barrier. [FJ]

REFERENCES

1. Prusiner, S. B. (1998) Prions. *Proc. Natl. Acad. Sci. USA* **95,** 13363–13383

2. Ronga, L., Tizzano, B., Palladino, P., Ragone, R., Urso, E., Maffia, M., Ruvo, M., Benedetti, E., and Rossi, F. (2006) The prion protein: Structural features and related toxic peptides. *Chem. Biol. Drug Design* **68,** 139–147

3. Weissmann, C., Fischer, M., Raeber, A., Bueler, H., Sailer, A., Shmerling, D., Rulicke, T., Brandner, S., and Aguzzi, A. (1996) The role of PrP in pathogenesis of experimental scrapie. *Cold Spring Harbor Symp. Quant. Biol.* **61,** 511–522

4. Griffith, J. S. (1967) Self-replication and scrapie. *Nature* **215,** 1043–1044

5. Alper, T., Cramp, W. A., Haig, D. A., and Clarke, M. C. (1967) Does the agent of scrapie replicate without nucleic acid? *Nature* **214,** 764–766

6. Bolton, D. C., McKinley, M. P., and Prusiner, S. B. (1982) Identification of a protein that purifies with the scrapie prion. *Science* **218,** 1309–1311

7. Govaerts, C., Wille, H., Prusiner, S. B., and Cohen, F. E. (2004) Evidence for assembly of prions with left-handed beta-helices into trimers. *Proc. Natl. Acad. Sci. USA* **101,** 8342–8347

8. Armen, R. S., DeMarco, M. L., Alonso, D. O., and Daggett, V. (2004) Pauling and Corey's alpha-pleated sheet structure may define the prefibrillar amyloidogenic intermediate in amyloid disease. *Proc. Natl. Acad. Sci. USA* **101,** 11622–11627

9. Ferguson, N., Becker, J., Tidow, H., Tremmel, S., Sharpe, T. D., Krause, G., Flinders, J., Petrovich, M., Berriman, J., Oschkinat, H., *et al.* (2006) General structural motifs of amyloid protofilaments. *Proc. Natl. Acad. Sci. USA* **103,** 16248–16253

10. Kuwata, K., Matumoto, T., Cheng, H., Nagayama, K., James, T. L., and Roder, H. (2003) NMR-detected hydrogen exchange and molecular dynamics simulations provide structural insight into fibril formation of prion protein fragment 106–126. *Proc. Natl. Acad. Sci. USA* **100,** 14790–14795

11. Laurent, M. (1998) Bistability and the species barrier in prion diseases: stepping across the threshold or not. *Biophys. Chem.* **72,** 211–222

12. Bishop, M. T., Hart, P., Aitchison, L., Baybutt, H. N., Plinston, C., Thomson, V., Tuzi, N. L., Head, M. W., Ironside, J. W., Will, R. G., *et al.* (2006) Predicting susceptibility and incubation time of human-to-human transmission of vCJD. *Lancet Neurol.* **5,** 393–398

13. Windl, O., Buchholz, M., Neubauer, A., Schulz-Schaeffer, W., Groschup, M., Walter, S., Arendt, S., Neumann, M., Voss, A. K., and Kretzschmar, H. A. (2005) Breaking an absolute species barrier: transgenic mice expressing the mink PrP gene are susceptible to transmissible mink encephalopathy. *J. Virol.* **79,** 14971–14975

14. Scott, M. R., Peretz, D., Nguyen, H. O., Dearmond, S. J., and Prusiner, S. B. (2005) Transmission barriers for bovine, ovine, and human prions in transgenic mice. *J. Virol.* **79,** 5259–5271

15. Bruce, M., Chree, A., McConnell, I., Foster, J., Pearson, G., and Fraser, H. (1994) Transmission of bovine spongiform encephalopathy and scrapie to mice: strain variation and the species barrier. *Philosoph. Trans.R. Soc. London* **343,** 405–411

16. Billeter, M., Riek, R., Wider, G., Hornemann, S., Glockshuber, R., and Wuthrich, K. (1997) Prion protein NMR structure and species barrier for prion diseases. *Proc. Natl. Acad. Sci. USA* **94,** 7281–7285

17. Calzolai, L., Lysek, D. A., Guntert, P., von Schroetter, C., Riek, R., Zahn, R., and Wuthrich, K. (2000) NMR structures of three single-residue variants of the human prion protein. *Proc. Natl. Acad. Sci. USA* **97,** 8340–8345

18. Calzolai, L., Lysek, D. A., Perez, D. R., Guntert, P., and Wuthrich, K. (2005) Prion protein NMR structures of chickens, turtles, and frogs. *Proc. Natl. Acad. Sci. USA* **102,** 651–655

19. Gossert, A. D., Bonjour, S., Lysek, D. A., Fiorito, F., and Wuthrich, K. (2005) Prion protein NMR structures of elk and of mouse/elk hybrids. *Proc. Natl. Acad. Sci. USA* **102,** 646–650

20. Lysek, D. A., Schorn, C., Nivon, L. G., Esteve-Moya, V., Christen, B., Calzolai, L., von Schroetter, C., Fiorito, F., Herrmann, T., Guntert, P., et al. (2005) Prion protein NMR structures of cats, dogs, pigs, and sheep. *Proc. Natl. Acad. Sci. USA* **102,** 640–645

21. Lopez Garcia, F., Zahn, R., Riek, R., and Wuthrich, K. (2000) NMR structure of the bovine prion protein. *Proc. Natl. Acad. Sci.USA* **97,** 8334–8339

22. Donne, D. G., Viles, J. H., Groth, D., Mehlhorn, I., James, T. L., Cohen, F. E., Prusiner, S. B., Wright, P. E., and Dyson, H. J. (1997) Structure of the recombinant full-length hamster prion protein PrP(29–231): the N terminus is highly flexible. *Proc. Natl. Acad. Sci. USA* **94,** 13452–13457

23. Zahn, R., Liu, A., Luhrs, T., Riek, R., von Schroetter, C., Lopez Garcia, F., Billeter, M., Calzolai, L., Wider, G., and Wuthrich, K. (2000) NMR solution structure of the human prion protein. *Proc. Natl. Acad. Sci. USA* **97,** 145–150

24. Riek, R., Wider, G., Billeter, M., Hornemann, S., Glockshuber, R., and Wuthrich, K. (1998) Prion protein NMR structure and familial human spongiform encephalopathies. *Proc. Natl. Acad. Sci. USA* **95,** 11667–11672

25. Raymond, G. J., Bossers, A., Raymond, L. D., O'Rourke, K. I., McHolland, L. E., Bryant, P. K., 3rd, Miller, M. W., Williams, E. S., Smits, M., and Caughey, B. (2000) Evidence of a molecular barrier limiting susceptibility of humans, cattle and sheep to chronic wasting disease. *EMBO J.* **19,** 4425–4430

26. Williams, E. S., and Miller, M. W. (2003) Transmissible spongiform encephalopathies in non-domestic animals: origin, transmission and risk factors. *Revue. Scientifique Technique (International Office of Epizootics)* **22,** 145–156

27. Kaneko, K., Zulianello, L., Scott, M., Cooper, C. M., Wallace, A. C., James, T. L., Cohen, F. E., and Prusiner, S. B. (1997) Evidence for protein X binding to a discontinuous epitope on the cellular prion protein during scrapie prion propagation. *Proc. Natl. Acad. Sci. USA* **94,** 10069–10074

28. Korth, C., Stierli, B., Streit, P., Moser, M., Schaller, O., Fischer, R., Schulz-Schaeffer, W., Kretzschmar, H., Raeber, A., Braun, U., *et al.* (1997) Prion (PrPSc)-specific epitope defined by a monoclonal antibody. *Nature* **390,** 74–77

29. Gorfe, A. A., Ferrara, P., Caflisch, A., Marti, D. N., Bosshard, H. R., and Jelesarov, I. (2002) Calculation of protein ionization equilibria with conformational sampling: pK(a) of a model leucine zipper, GCN4 and barnase. *Proteins* **46,** 41–60

30. MacKerell, A. D., Bashford, D., Bellott, M., Dunbrack, R. L., Evanseck, J. D., Field, M. J., Fischer, S., Gao, J., Guo, H., Ha, S., *et al.* (1998) All-atom empirical potential for molecular modeling and dynamics studies of proteins. *J. Phys. Chem. B.* **102,** 3586–3616

31. Brooks, B. R., Bruccoleri, R. E., Olafson, B. D., States, D. J., Swaminathan, S., and Karplus, M. (1983) Charmm—a program for macromolecular energy, minimization, and dynamics calculations. *J. Comp. Chem.* **4,** 187–217

32. Phillips, J. C., Braun, R., Wang, W., Gumbart, J., Tajkhorshid, E., Villa, E., Chipot, C., Skeel, R. D., Kale, L., and Schulten, K. (2005) Scalable molecular dynamics with NAMD. *J. Comp. Chem.* **26,** 1781–1802

33. Gorfe, A. A., and Caflisch, A. (2005) Functional plasticity in the substrate binding site of beta-secretase. *Structure* **13,** 1487–1498

34. Santini, S., and Derreumaux, P. (2004) Helix H1 of the prion protein is rather stable against environmental purturbations: molcular dynamics of mutation and deletion variants of PrP(90–231) CMLS. *Cell Mol. Life Sci.* **61,** 951–960

35. Gsponer, J., Ferrara, P., and Caflisch, A. (2001) Flexibility of the murine prion protein and its Asp178Asn mutant investigated by molecular dynamics simulations. *J. Mol. Graphics Model.* **20,** 169–182

36. Dima, R. I., and Thirumalai, D. (2002) Exploring the propensities of helices in PrP(C) to form beta sheet using NMR structures and sequence alignments. *Biophys. J.* **83,** 1268–1280

37. McGaughey, G. B., Gagne, M., and Rappe, A. K. (1998) pi-Stacking interactions. Alive and well in proteins. *J. Biol. Chem.* **273,** 15458–15463

38. Miller, M. W., and Williams, E. S. (2004) Chronic wasting disease of cervids. *Curr. Topics Microbiol. Immunol.* **284,** 193–214

39. Miller, M. W., Wild, M. A., and Williams, E. S. (1998) Epidemiology of chronic wasting disease in captive Rocky Mountain elk. *J. Wildlife Dis.* **34,** 532–538

40. Miller, M. W., Williams, E. S., McCarty, C. W., Spraker, T. R., Kreeger, T. J., Larsen, C. T., and Thorne, E. T. (2000) Epizootiology of chronic wasting disease in free-ranging cervids in Colorado and Wyoming. *J. Wildlife Dis.* **36,** 676–690

41. O'Rourke, K. I., Besser, T. E., Miller, M. W., Cline, T. F., Spraker, T. R., Jenny, A. L., Wild, M. A., Zebarth, G. L., and Williams, E. S. (1999) PrP genotypes of captive and free-ranging Rocky Mountain elk (*Cervus elaphus nelsoni*) with chronic wasting disease. *J. Gen. Virol.* **80 (Pt 10),** 2765–2769

42. Miller, M. W., and Williams, E. S. (2002) Detection of PrP(CWD) in mule deer by immunohistochemistry of lymphoid tissues. *Vet. Rec.* **151,** 610–612

43. Fox, K. A., Jewell, J. E., Williams, E. S., and Miller, M. W. (2006) Patterns of PrPCWD accumulation during the course of chronic wasting disease infection in orally inoculated mule deer (*Odocoileus hemionus*). *J. Gen. Virol.* **87,** 3451–3461

44. Miller, M. W., Williams, E. S., Hobbs, N. T., and Wolfe, L. L. (2004) Environmental sources of prion transmission in mule deer. *Emerg. Infect. Dis.* **10,** 1003–1006

45. Williams, E. S., and Miller, M. W. (2002) Chronic wasting disease in deer and elk in North America. *Revue Scientifique Technique. (International Office of Epizootics)* **21,** 305–316

46. Belay, E. D., Maddox, R. A., Williams, E. S., Miller, M. W., Gambetti, P., and Schonberger, L. B. (2004) Chronic wasting disease and potential transmission to humans. *Emerg. Infect. Dis.* **10,** 977–984

47. Goldmann, W., Houston, F., Stewart, P., Perucchini, M., Foster, J., and Hunter, N. (2006) Ovine prion protein variant A136R154L168Q171 increases resistance to experimental challenge with bovine spongiform encephalopathy agent. *J. Gen. Virol.* **87,** 3741–3745

48. Eghiaian, F., Grosclaude, J., Lesceu, S., Debey, P., Doublet, B., Treguer, E., Rezaei, H., and Knossow, M. (2004) Insight into the PrPC–>PrPSc conversion from the structures of antibody-bound ovine prion scrapie-susceptibility variants. *Proc. Natl. Acad. Sci. USA* **101,** 10254–10259

49. Horiuchi, M., Baron, G. S., Xiong, L. W., and Caughey, B. (2001) Inhibition of interactions and interconversions of prion protein isoforms by peptide fragments from the C-terminal folded domain. *J. Biol. Chem.* **276,** 15489–15497

50. Alonso, D. O., DeArmond, S. J., Cohen, F. E., and Daggett, V. (2001) Mapping the early steps in the pH-induced conformational conversion of the prion protein. *Proc. Natl. Acad. Sci.USA* **98,** 2985–2989

51. Bruce, M. E. (2000) 'New variant' Creutzfeldt-Jakob disease and bovine spongiform encephalopathy. *Nat. Med.* **6,** 258–259